Giant Magellan Telescope Adaptive Optics Overview

Antonin H. Bouchez*[a], Laird M. Close[b], Rodolphe Conan[a], Richard Demers[a], Simone Esposito[c], Frank Groark[a], Jared Males[b], Brian. A. McLeod[d], Fernando Quirós-Pacheco[a], Rob Sharp[e], Breann N. Sitarski[f], Peter Thompson[a], Marcos A. van Dam[g]
[a]GMTO Corporation, 300 N. Lake Ave., 14th Floor, Pasadena, CA 91101, USA; [b]Steward Observatory, 933 N. Cherry Ave., Tucson, AZ 85719, USA; [c]INAF-Arcetri, Largo E. Fermi 5, Firenze 50125, Italy; [d]Smithsonian Astrophysical Observatory, 60 Garden St, Cambridge, MA 02138, USA; [e]RSAA, The Australian National University, Cotter Road, Weston Creek, ACT 2611, Australia; [f] NASA Goddard Space Flight Center, 880 Greenbelt Rd., Greenbelt, MD 20771, USA; [g]Flat Wavefronts, 21 Lascelles Street, Christchurch 8022, New Zealand

ABSTRACT

The 25.4 m diameter Giant Magellan Telescope will have four first-generation observing modes: Natural seeing, ground-layer AO, natural guide star AO, and laser tomography AO. These control modes are enabled by a suite of wavefront sensors and metrology systems that provide feedback to a segmented active primary mirror and a segmented adaptive secondary mirror. There have been several changes made to the GMT AO design since the last conference. The Natural Guide Star Wavefront Sensor now incorporates both a pyramid wavefront sensor for high-order sensing and a Holographic Dispersed Fringe Sensor to increase the segment piston sensing dynamic range. The On-Instrument Wavefront Sensors of the GMTNIRS and GMTIFS instruments have been further developed and now include real-time phase retrieval to sense segment piston errors at high frame rate. We are developing laboratory optical testbeds and prototype wavefront sensors to validate active optics and AO algorithms. We are also fabricating the first off-axis adaptive secondary mirror segment to retire fabrication risk and verify its performance.

Keywords: Extremely Large Telescopes, Wavefront Sensing, Laser Guide Stars, Segment Phasing.

1. INTRODUCTION

1.1 GMT Optical Design and Instruments

The Giant Magellan Telescope (GMT) is an aplanatic Gregorian telescope whose primary mirror (M1) is composed of seven 8.4 m diameter circular segments with active position and figure control (Figure 1) [1]. The secondary mirror (M2) is composed of seven 1.05 m diameter concave circular segments with matching segmentation, conjugated to an altitude of 165 m above M1. Two versions of the secondary mirror will be available: An adaptive secondary mirror with high-order and high-bandwidth figure control, and a fast-steering secondary mirror composed of rigid segments. A tertiary mirror (M3) can be inserted ahead of the direct Gregorian focus to direct a 3 arcmin diameter field to narrow-field instruments. A refractive field corrector and atmospheric dispersion compensator (C-ADC) can be inserted on the telescope optical axis to improve image quality over a field of view up to 20 arcmin diameter for wide-field instruments.

The GMT optics are supported by an altitude-over-azimuth Mount [2], leading to apparent rotation of the sky at the telescope focus as the Mount tracks the Earth's rotation. The apparent sky rotation is compensated by a single Gregorian Instrument Rotator (GIR) to which the instruments and wavefront sensors are mounted. Wide-field, seeing-limited scientific instruments are located at the direct Gregorian focus (DG) after only two reflections (M1 and M2). Diffraction-limited instruments are located at the folded port focus (FP) after reflection off M3.

*abouchez@gmto.org; phone +1 626 204 0517

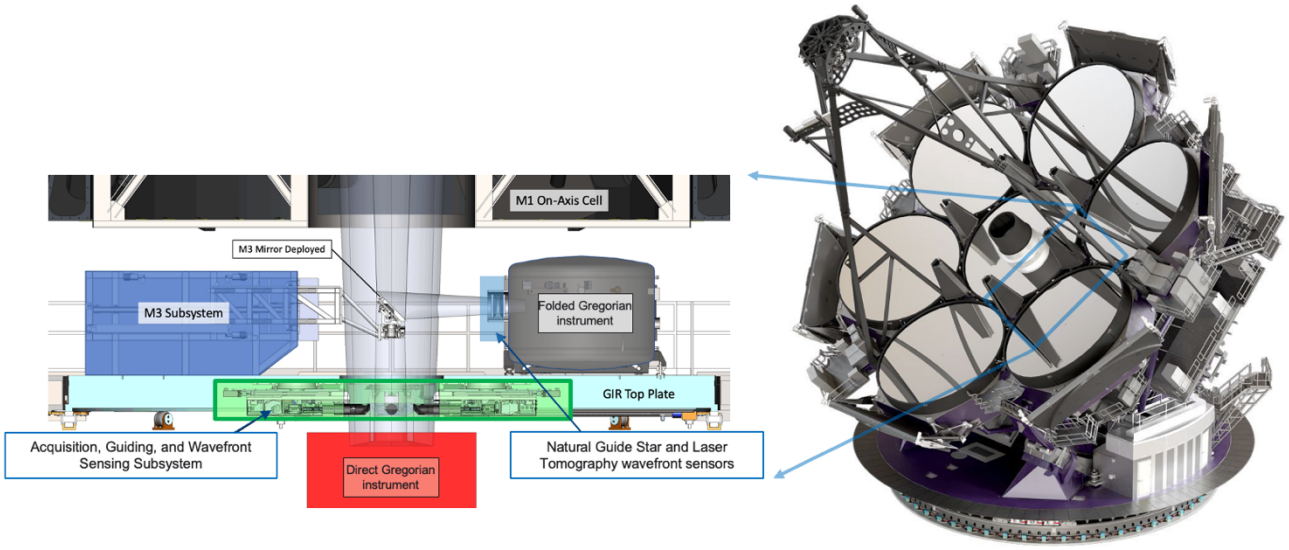

Figure 1: Rendering of the GMT (*right*) with a cross-section of the region below the M1 on-axis cell (*left*) illustrating the M3 mirror, the Acquisition, Guiding, and Wavefront Sensing Subsystem below it, and two instruments mounted to the Gregorian Instrument Rotator.

The first-generation of scientific instruments will include three seeing-limited instruments that will benefit from Ground Layer AO correction, and three diffraction-limited instruments:

- G-CLEF: 0.35-0.90 µm R=20,000-100,000 single-object seeing-limited spectrograph [3]
- GMACS: 0.33-1.0 µm R=1000-6000 multi-object seeing-limited spectrograph [4]
- MANIFEST: 0.35-1.0 µm robotic fiber positioner to feed G-CLEF and GMACS over a 20 arcmin field [5]
- GMTIFS: 0.95-2.5 µm R=10,000 diffraction-limited integral field spectrograph and imager [6]
- GMTNIRS: 1.1-5.3 µm R=50,000 diffraction-limited single-object spectrograph [7]
- GMagAO-X: 0.6-1.7 µm coronagraphic diffraction-limited imager and spectrograph [8]

A visible light Commissioning Camera [9] and a near-infrared AO Test Camera are also planned.

1.2 Wavefront Control Modes

The GMT incorporates both active optics (AcO, active control of telescope optics to compensate for slow alignment and figure errors) and adaptive optics (AO, correcting for high-frequency atmospheric and telescope phase errors) to deliver the best possible image quality to its scientific instruments. The broad range of GMT science goals and constraints imposed by the Earth's atmosphere motivate a range of wavefront control strategies that trade off image quality, field of view, sky coverage, and development risk. Four wavefront control modes will be implemented for the first generation of GMT instruments:

Natural Seeing (NS): The Natural Seeing mode is the only mode available when the fast-steering secondary mirror is installed. It provides a low-risk wavefront control mode for telescope commissioning, and a backup capability during periods when the adaptive secondary mirror (ASM) is removed for maintenance. Only misalignments of the M1 and M2 segments and low-order figure errors of the M1 segments are actively controlled, including segment tip-tilt vibrations up to 2.5 Hz. No attempt is made to correct atmospheric wavefront error or telescope segment phasing error.

Ground Layer AO (GLAO): The GLAO mode provides improved resolution and sensitivity for medium and wide-field instruments by compensating low-altitude atmospheric wavefront error using the ASM. The resulting images are seeing-limited, but with a 5-50% reduction in image size with respect to Natural Seeing, depending on the corrected field of view and observing wavelength. Telescope segment phasing is not required in this mode.

Natural Guide Star AO (NGAO): The NGAO mode is used for high spatial resolution imaging and spectroscopy of bright objects, and high-contrast science programs. The light of a single bright natural guide star (NGS) is used to measure the on-axis atmospheric and telescope wavefront error, which are compensated by the ASM. This includes high-bandwidth

control of telescope segment phasing errors. The resulting point spread function is diffraction-limited in the visible and near-infrared over a field of view limited by atmospheric anisoplanatism.

Laser Tomography AO (LTAO): The LTAO mode enables high spatial resolution imaging and spectroscopy of faint objects in the near-infrared, with high sky coverage. An asterism of laser guide stars (LGS) is used to tomographically reconstruct the high-order components of the atmospheric and telescope wavefront error in the direction of a science target, while one faint NGS is used to measure low-order aberrations and segment phasing errors. This control mode provides a diffraction-limited PSF in the near-infrared over a field of view limited by atmospheric anisoplanatism.

1.3 Image Quality Requirements

The GMT Science Requirements Document and Concept of Operations at Level 1 of the GMT requirements tree specify the image quality required to achieve the science and operational goals of the observatory. For seeing-limited observing cases, these are defined in terms of PSF full-width at half maximum (FWHM) in the visible and near-infrared. For diffraction-limited observing cases, the metrics are Strehl ratio and the signal-to-noise ratio (SNR) achievable on high-contrast targets in the near-infrared. The science requirements must be met in the best environmental conditions of the site, while the ConOps requirements must be met at least 75% of the time. These Level 1 image quality requirements are summarized in Table 1.

Table 1: Level 1 image quality requirements

Observing Cases	ID	Requirement
Seeing-Limited	ConOps-45913C	FWHM(0.5 μm) < 1.20× the natural seeing over a 10′ diam. field ≥ 75% of the time
	ConOps-45913D	FWHM(1.65 μm) < 1.25× the natural seeing over a 10′ diam. field ≥ 75% of the time
	ConOps-45913E	FWHM(0.5 μm) < 1.25× the natural seeing over a 20′ diam. field ≥ 75% of the time
	REQ-L1-SCI-23241	FWHM(0.5 μm) < 0.30 arcsec over a 10′ diam. field in best conditions
	REQ-L1-SCI-23265	FWHM(1.65 μm) < 0.20 arcsec over a 10′ diam. field in best conditions
	REQ-L1-SCI-23295	FWHM(0.5 μm) < 0.35 arcsec over a 20′ diam. field in best conditions
Diffraction-Limited	REQ-L1-SCI-23201	Strehl(1.65 μm) ≥ 75% on-axis when using a bright guide star in best conditions
	REQ-L1-SCI-23165	Strehl(1.65 μm) ≥ 50% with ≥ 80% sky coverage in best conditions
	REQ-L1-SCI-23203	SNR ≥ 5 at 3.8 μm in 3600 s on a companion with flux ratio of 10^5 at 120 mas separation from a bright star in best conditions

The science requirements have been flowed down to the technical requirements on the observatory specified in the Observatory Requirements Document (Level 2) and Observatory Architecture Document (OAD, Level 3). The best conditions of the science requirements are interpreted as 5th percentile atmospheric wavefront error at the GMT site and an absence of wind-induced errors. The science requirements can thereby be converted to the equivalent image quality that would be achieved in median conditions with the same telescope wavefront errors. Seeing-limited FWHM requirements (both natural seeing and GLAO-corrected) are converted to the equivalent Normalized Point Source Sensitivity (PSSN) to enable analytic performance budgets to be developed. The PSSN metric quantifies the reduction in point source sensitivity of the aberrated telescope compared to that of a perfect telescope without ground-layer correction at the same site. Diffraction-limited requirements are specified in terms of the residual wavefront error (WFE). The Level 1 contrast requirement has been demonstrated to be consistent with the ≤ 173 nm RMS WFE NGAO WFE requirement.

Table 2: Level 3 image quality requirements

WFC Mode	ID	Requirement
NS	REQ-L3-OAD-80213	PSSN(0.5 μm) ≥ 0.7765 on-axis, with ≥ 99% sky coverage
	REQ-L3-OAD-80213	PSSN(1.65 μm) ≥ 0.7450 on-axis, with ≥ 99% sky coverage
	REQ-L3-OAD-TBD	PSSN(0.5 μm) ≥ 0.7311 on-axis, with ≥ 99% sky coverage
GLAO	REQ-L3-OAD-80222	PSSN(0.5 μm) ≥ 1.7351 on-axis, with ≥ 99% sky coverage
	REQ-L3-OAD-80222	PSSN(1.65 μm) ≥ 1.6855 on-axis, with ≥ 99% sky coverage
	REQ-L3-OAD-TBD	PSSN(0.5 μm) ≥ 1.5194 over a 20′ diam. field of view, with ≥ 99% sky coverage
NGAO	REQ-L3-OAD-80223	RMS WFE ≤ 173 nm RMS on-axis when using an R=10 guide star
LTAO	REQ-L3-OAD-96756	RMS WFE ≤ 340 nm RMS on-axis with ≥ 80% sky coverage
	REQ-L3-OAD-118339	RMS WFE ≤ 340 nm RMS on-axis using K≤14 on-axis guide stars

The Level 3 image quality requirements are specified as the *median* observatory performance over a representative ensemble of observing scenarios and environmental conditions. These requirements, together with architectural design choices described in the OAD, form the basis of the image quality budgets used to flow down performance requirements to the subsystems that compose the wavefront control system.

2. ACTIVE OPTICS AND GLAO

2.1 Telescope Metrology System

The Telescope Metrology System (TMS) measures the positions of all primary optics, wavefront sensors, and instruments on the GMT to enable rapid alignment to within the capture range of the wavefront sensors in all wavefront control modes [10]. It consists of a Laser Tracker Network (LTN) for initial alignment with large capture range and a fixed Laser Metrology Truss (LMT) between the M1 and M2 segments to maintain alignment during operation (Figure 2).

The Laser Tracker Network consists of three Leica AT930 laser trackers mounted to the M2 truss, one mounted below the M1 on-axis segment, and numerous retroreflectors. These can measure the positions of M1, M2, M3, the C-ADC, wavefront sensors, and instruments in a fixed reference frame defined by wide-angle retroreflectors on the Enclosure floor. The LTN will be used for initial installation of all optical subsystems and developing flexure and pointing models.

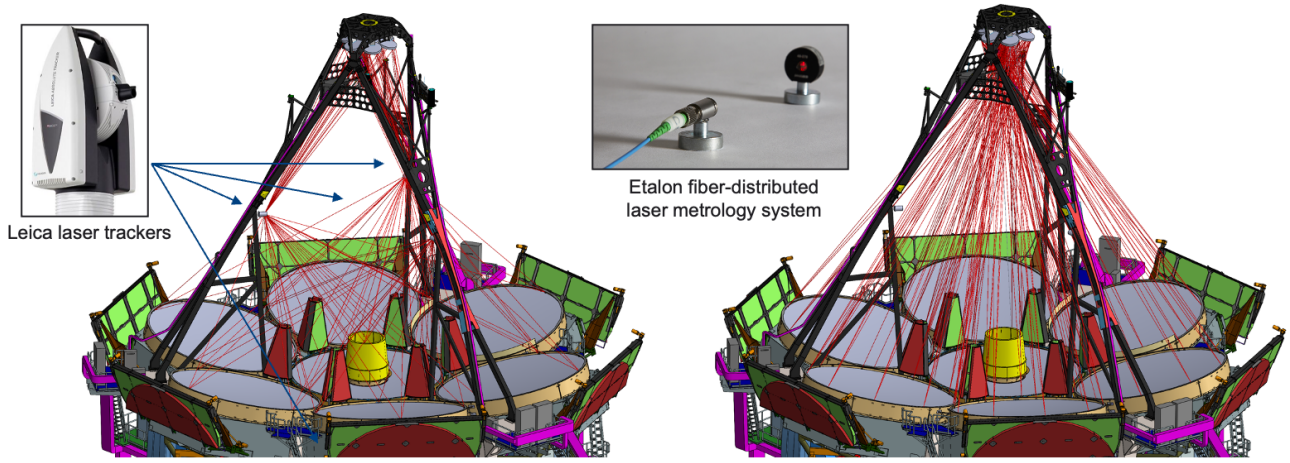

Figure 2: TMS Laser Tracker Network (*left*) and Laser Metrology Truss (*right*) measurement baselines shown in red. The M1 and M2 edge sensor baselines are hidden.

While providing great flexibility, optics position determination with the LTN is time-consuming and insufficiently accurate to ensure that light falls within the capture ranges of all wavefront sensors. A higher-precision metrology system with smaller dynamic range is used to bridge this gap. The Laser Metrology Truss consists of 159 fixed measurement baselines between laser collimators and retroreflectors mounted on the M1 and M2 segments. In its absolute measurement mode, the LMT uses an Etalon Absolute Multiline Technology laser unit to measure the length of each of these baselines to <0.5 parts per million in < 15 seconds. This allows the Observatory Control System (OCS) to return the primary optics to pre-calibrated relative positions within the capture ranges of the wavefront sensors after each slew.

The LMT fulfills an additional function in the NGAO and LTAO wavefront control modes. In its differential measurement mode, the 96 baselines spanning the M1 segment gaps and the M2 segment gaps are measured by Attocube IDS3010 differential interferometers, using the same fibers, collimators, and retroreflectors. The Attocube interferometers measure the relative displacement between segments at high bandwidth (≥500 Hz) and precision (<25 nm RMS in segment piston). These measurements supplement those made by the adaptive optics wavefront sensors, enabling the compensation of high-frequency segment vibrations.

2.2 Acquisition, Guiding, and Wavefront Sensing Subsystem

The Acquisition, Guiding, and Wavefront Sensing Subsystem (AGWS) is the first stage telescope wavefront sensing system, used in all wavefront control modes and with all science instruments [11]. It keeps the optics of the GMT coaligned, conforming to the correct shape, and phased by simultaneously sensing the light of three or four off-axis natural

guide stars. The AGWS is the primary wavefront sensing system when operating in the NS and GLAO wavefront control modes. In the NGAO and LTAO modes, it fulfills the initial acquisition and alignment function, including initial phasing of the seven segment pairs. In all wavefront control modes, the AGWS continues to drive active optics corrections, minimizing field dependent aberrations due to segment misalignments and deformation.

The AGWS consists of four independent wavefront sensing probes that patrol the Direct Gregorian focal surface (Figure 3). At least one probe can reach any guide star between 3′ and 10′ field angle. Each probe can also reach the on-axis position for calibration purposes.

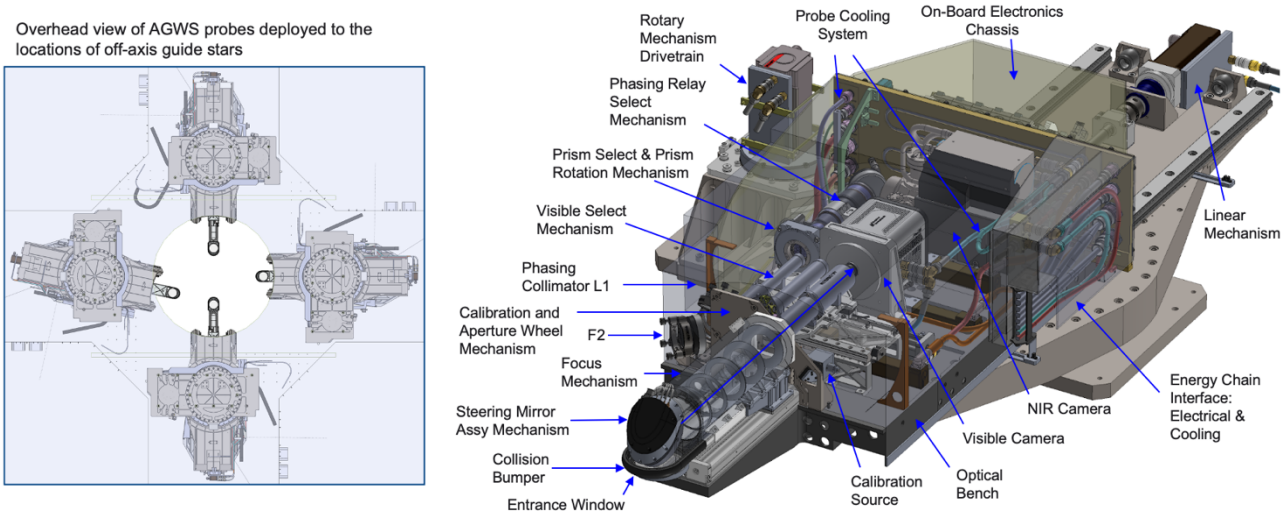

Figure 3: (*Left*) Overhead view of AGWS probes. (*Right*) AGWS probe detailed design.

Each AGWS probe has two optical channels: a visible channel using 600-900 nm wavelength light that fulfills the acquisition, guiding and wavefront sensing functions, and a near-IR channel using 1027-1358 nm wavelength light that fulfills the segment phasing function. The visible channel can operate in one of three configurations, using an actuated mechanism to place the appropriate set of optics in the beam in front of a fixed 1024×1024 pixel Electron-Multiplication Charge Coupled Device (EMCCD) camera (Figure 4).

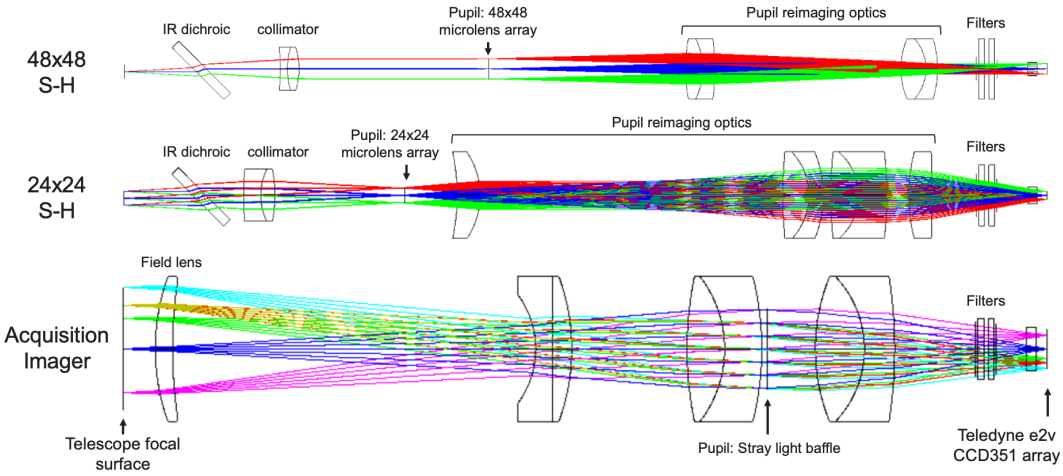

Figure 4: AGWS visible channel optical configurations.

Both wavefront sensor configurations of the visible channel include a tilted dichroic after the field stop that directs light with wavelength longer than 950 nm to the infrared dispersed fringe sensor (DFS), which fulfills the initial segment phasing function. This segment piston measurement capability is available anytime the wavefront sensors are in use, but we currently intend to use these measurements only when in the NGAO and LTAO control modes. The DFS operates by

forming a pupil image onto a mask that isolates 1.5 m square subapertures that span the 12 tangent points between the segments (Figure 5). Immediately after going through the mask, the light passes through an array of prisms and lenses and is dispersed and focused. A phase difference between adjacent segments is manifested as a tilt in the resulting dispersed fringes, recorded by a SAPHIRA 256×320 pixel electron-multiplication avalanche photodiode (eAPD) array. Six calibration apertures, located entirely within off-axis segments, enable systematic errors such those caused by varying atmospheric dispersion to be detected and corrected.

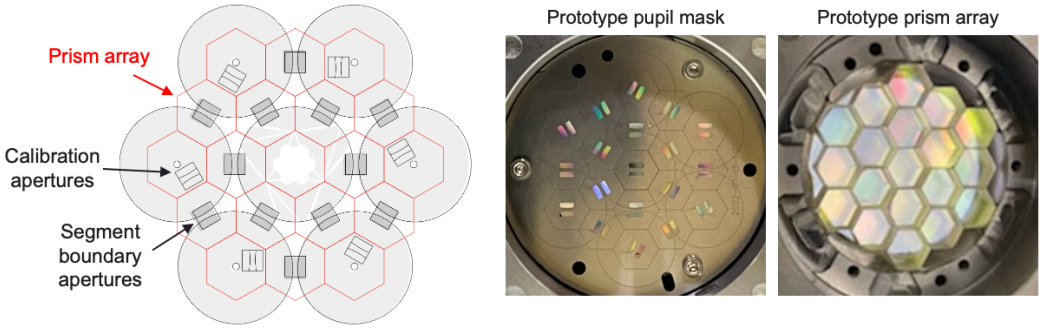

Figure 5: (*Left*) The AGWS DFS prism array (red outline) and apertures (dark gray) overlayed on the GMT pupil. (*Right*) Prototype pupil mask and prism array installed in AGWS Probe Zero.

2.3 Wide Field Phasing Testbed

The GMT project has partnered with the Smithsonian Astrophysical Observatory to build a laboratory optical testbed to verify the design of the GMT active optics wavefront sensors and control algorithms [12]. This includes demonstrating initial target acquisition, segment stacking, active optics control, and segment phasing control over a wide field of view, from an initial misaligned state. The Wide Field Phasing Testbed (WFPT) consists of a set of optical relays in which are located segmented and deformable mirrors that represent the GMT M1 and M2 mirrors (Figure 6, left). The testbed output beam has the GMT's f/8.16 focal ratio and a sufficient back focal distance to send light into a full-scale prototype of one AGWS probe (Figure 6, right). Over its 20 mm diameter field of view, the testbed produces the field-dependent aberrations due to misalignment corresponding to those that would occur over the 20 arcminute field of the GMT. A rotating phase plate generates seeing-limited images that correspond to typical atmospheric conditions expected at the GMT.

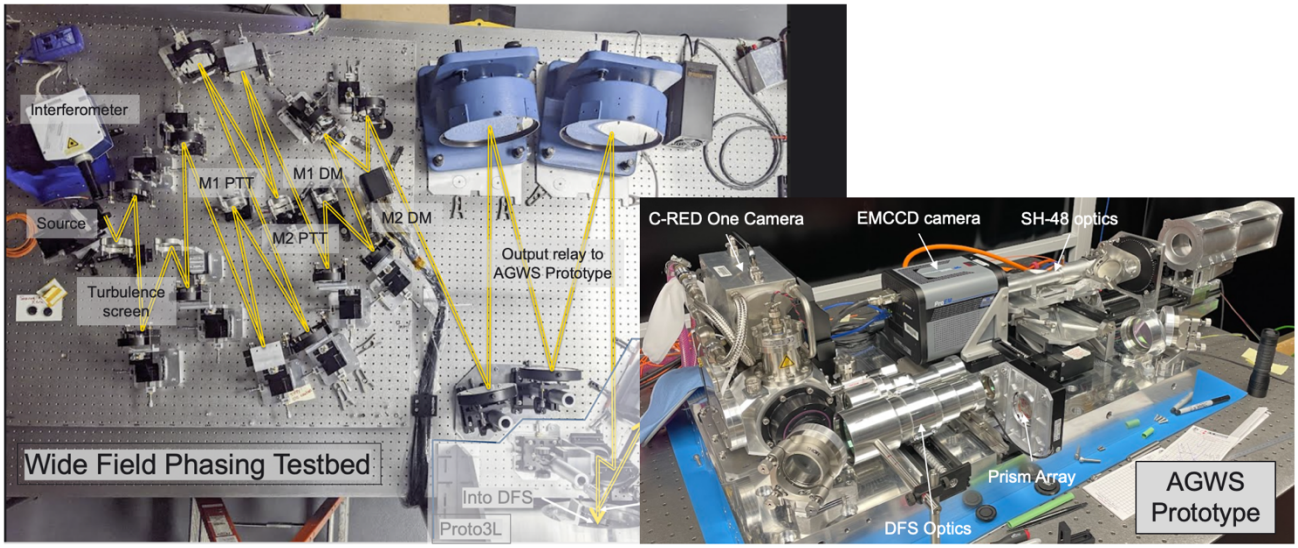

Figure 6: (*Left*) Overhead view of the Wide Field Phasing Testbed. (*Right*) The AGWS prototype probe prior to installation.

On the telescope, the AGWS will have four identical probes operating simultaneously on four different stars to sample the field-dependent aberrations. On the testbed, the AGWS Prototype is positioned sequentially to four off-axis positions without changing the state of the testbed optics. Those measurements are combined as if they came from four separate

probes before generating corrections to the testbed optics. Verification of the active optics and initial segment phasing performance is currently underway.

3. ADAPTIVE SECONDARY MIRROR

3.1 Design

The GMT Adaptive Secondary Mirror (ASM) is being developed by the AdOptica consortium consisting for Microgate Corp. and ADS International [13]. The ASM is composed of 7 independent 1.05 m diameter segments, each with 675 voice coil actuators supporting a thin Zerodur face sheet for figure control (Figure 7). There are a total of 4725 actuators with a mean projected spacing at M1 of 28.5 cm. The face sheet figure can be updated at up to 2 kHz with a -3 dB bandwidth of 800 Hz. Each segment is supported by a 6 degree of freedom positioning system with a bandwidth of 2 Hz. Each ASM segment face sheet has sufficient stroke to simultaneously compensate worst-case atmospheric wavefront error (r_0=7 cm), wind-induced telescope vibrations at the limit of regular operating conditions (17 m/s wind speed), and M1 and M2 segment positioner errors, with 20% margin.

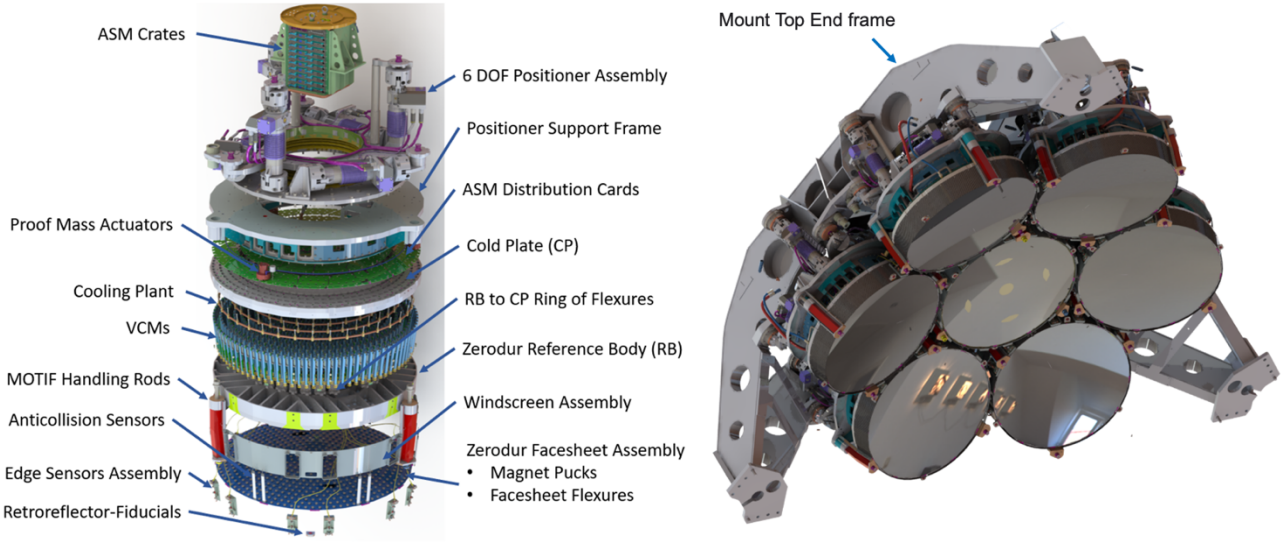

Figure 7: (*Left*) Exploded view of an ASM segment. (*Right*) Rendering of the ASM mounted on the Top End frame.

3.2 Fabrication Status

The first off-axis ASM segment is currently being manufactured by AdOptica and their subcontractors (Figure 8). The reference body, face sheet, and major structural components have been completed and will be integrated for structural dynamic testing later this year. After this, they will be used for full-scale tests of the M2 optical edge sensors. The face sheet, manufactured by Safran-Reosc, has achieved 8 nm surface figure error with 0.08 N flattening force, meeting requirements. The remaining components of the first segment will be manufactured in 2024, enabling the first segment to be electro-mechanically and optically tested in 2025-2026. Fabrication of the remaining 6 segments will begin in parallel with these activities.

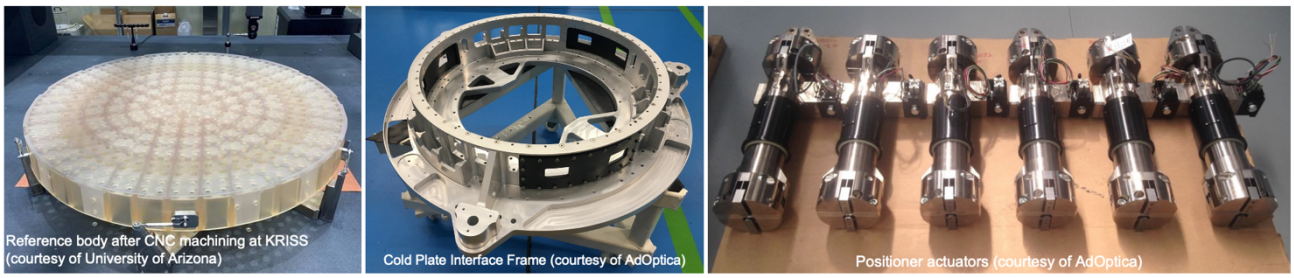

Figure 8: Components of the first off-axis adaptive secondary mirror segment.

4. NATURAL GUIDE STAR ADAPTIVE OPTICS

4.1 Introduction

The Natural Guide Star Adaptive Optics (NGAO) wavefront control mode delivers diffraction-limited, high-contrast images in the near-infrared for astronomical targets with nearby bright natural guide stars. It will be used primarily for high spatial and/or spectral resolution galactic and planetary observations, and for the characterization of nearby stellar companions and circumstellar environments. The light of a single bright guide star (R<16) provides the high-bandwidth wavefront sensing required to compensate atmospheric and telescope wavefront error. This star can be located up to 60″ off-axis, though atmospheric anisoplanatism becomes a dominant source of wavefront error if >5″.

The Natural Guide Star Wavefront Sensor Subsystem (NGWS) and Laser Tomography Wavefront Sensor Subsystem (LTWS) fulfill the high-order wavefront sensing function in the NGAO and LTAO wavefront control modes, respectively. The NGWS and LTWS are fed by light reflected off a dichroic instrument window (Figure 9, left). This architecture is referred to as a "direct feed" to the instruments, avoiding the added emissivity and throughput losses of a post-focal optical relay. The front surface of the instrument window reflects visible light (λ<930 nm for GMTIFS, λ<1000 nm for GMTNIRS) while infrared light is transmitted into the instrument. The visible beam next encounters a dichroic that reflects only a narrow band around 589 nm wavelength to the LTWS.

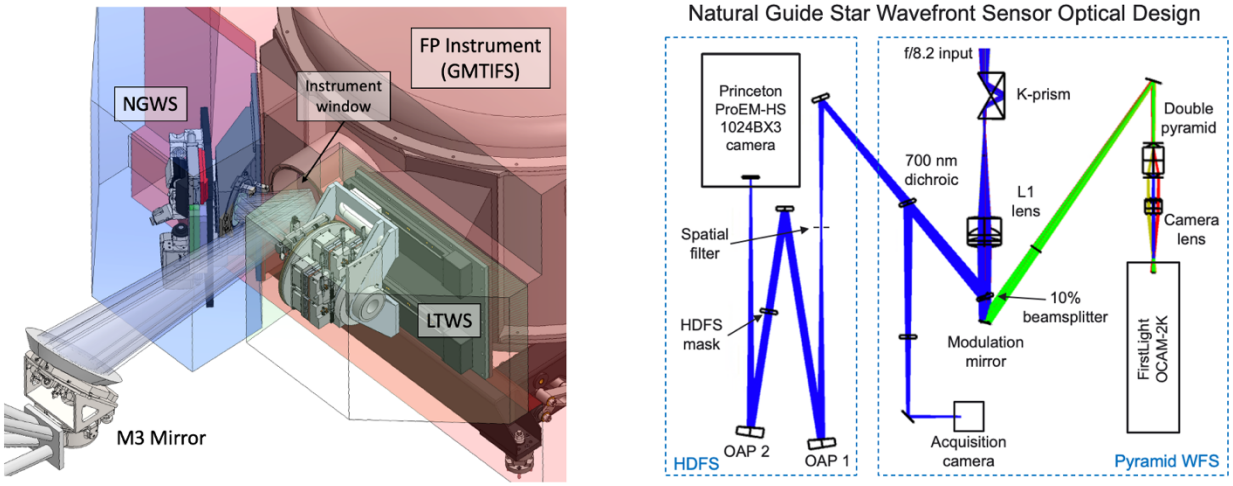

Figure 9: (*Left*) Natural and Laser Tomography wavefront sensors mounted to the front of the GMTIFS instrument (*Right*) Optical design of the NGWS prototype.

Two identical copies of the NGWS and LTWS are being developed. Unit 1 of each will initially be deployed with the AO Test Camera for laboratory performance verification with the ASM, first in AdOptica's test facility in Italy, then in the GMTO Summit Support Building, and finally for on-sky performance verification on the GMT. Unit 2 of each sensor will be installed on the GMTNIRS instrument prior to its installation on the telescope. Unit 1 of each sensor will eventually be transferred to the GMTIFS instrument before it is deployed in the operations phase.

4.2 Natural Guide Star Wavefront Sensor

The NGWS must sense all wavefront aberrations due to the atmosphere and telescope, including global tip-tilt, segment tip-tilt and piston, and high-order continuous modes across each segment. The need to sense segment piston at high bandwidth led to the selection of a pyramid wavefront sensor (PWFS), which also provides high sensitivity and low aliasing of high spatial frequencies. The PWFS relies on interference between the light of adjacent segments to measure segment phase piston error. It therefore has a sinusoidal response to segment piston error and is subject to phase wrapping errors when the phase difference between segments exceeds half of the sensing wavelength. A dedicated phasing sensor with larger dynamic range (at the expense of sensitivity and sampling rate) is required to detect occasional phase wrapping errors and restore the phased condition.

Several potential second phasing channel designs were considered in a trade study performed by INAF-Arcetri and GMTO [14] [15]. These included pyramid wavefront sensors in the visible and near-infrared, two configurations of Zernike

wavefront sensors, several configurations of phase retrieval sensors, and two types of dispersed fringe sensors. The Holographic Dispersed Fringe Sensor [16] (HDFS) was selected as the baseline design, with the LIFT technique to be further investigated as a backup design. The HDFS uses a phase mask in a pupil plane to selectively interfere GMT segment pairs in the next focal plane (Figure 10). The light from each GMT segment is transmitted through a multiplexed transmissive diffraction grating. The diffraction gratings are oriented in such a way that the spectra of segment pairs are superimposed and interfere with one another in the focal plane. The 14 images of the guide star formed in this way encode the average phase differences between segment pairs as a wavelength-dependence shifts in the interference patterns, which takes the form of a barber-pole pattern for phase differences > ±2π radians (Figure 10, right). The NGWS optical design is illustrated in Figure 9, right.

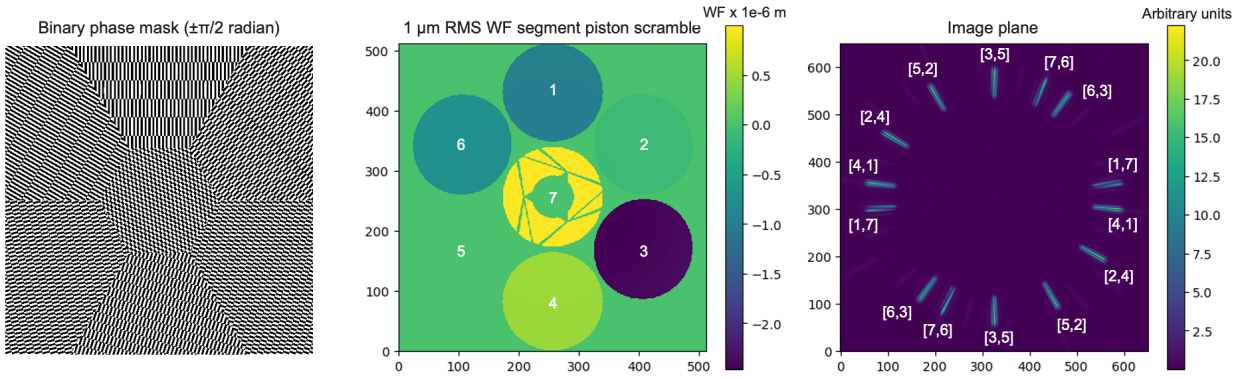

Figure 10: (*Left*) HDFS binary phase mask. (*Center*) Input phase errors with segment numbers identified. (*Right*) Resulting fringes in the image plane, with segment pairs identified.

4.3 High Contrast AO Testbed

The High Contrast AO Testbed (HCAT) is being developed in collaboration with the University of Arizona and INAF-Arcetri to verify the performance of the NGWS and planned NGAO control algorithms, while also testing the pupil splitting and coherent recombination design of GMagAO-X [18]. HCAT consists of a telescope simulator that generates a GMT-like beam, the MagAO-X instrument acting as a surrogate for the GMT ASM with 1500 actuators across the GMT pupil, and a full-scale NGWS prototype wavefront sensor (Figure 11).

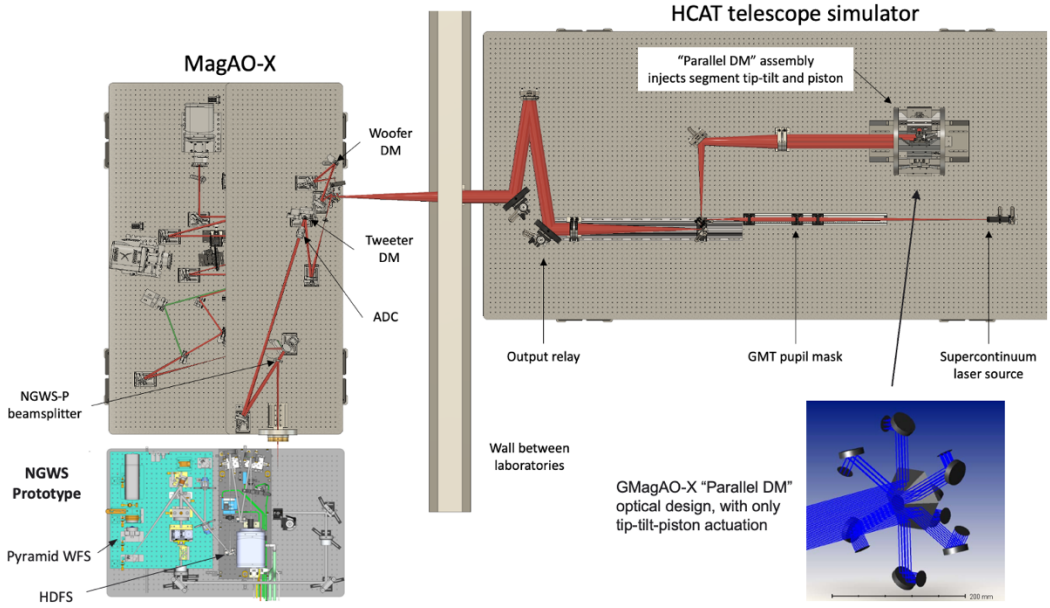

Figure 11: The High Contrast AO Testbed consists of a telescope simulator (left), the MagAO-X instrument (upper right), and a prototype of the GMT Natural Guide Star Wavefront Sensor (lower right).

The GMagAO-X instrument will split the GMT pupil onto seven 3000-actuator deformable mirrors and recombine the beams to achieve high Strehl and extreme contrast at visible wavelengths [8]. The same "Parallel DM" design has been incorporated into the HCAT telescope simulator, but with only piston, tip, and tilt actuation of each segment. The NGWS Prototype reproduces the preliminary optical design of the PWFS and HDFS channels, enabling the testing of all NGAO real-time control loops [19]. HCAT was integrated and commissioned in summer 2023, and testing is currently underway.

4.4 NGAO Expected Performance

The NGAO wavefront error budget (Figure 12, left) is used to flow down performance requirements to subsystems and compute the current best estimate (CBE) performance. CBEs highlighted in green are based on mature simulations or analysis that represents the current design, while values highlighted yellow are allocations, typically based on simple analytical models or analogy to existing AO systems. The mature estimates comprise 77% of the total variance. The current predicted wavefront error is 157.3 nm RMS, corresponding to a Strehl of 70% at 1.65 µm. This leaves a margin of 72.0 nm RMS against the Level 2 requirement of achieving Strehl(1.65 µm) ≥ 65%. The greatest uncertainties in this performance estimate are in the level of residual mechanical vibrations, aero-thermal errors (dome seeing and the "low-wind effect"), and calibration error terms. These error terms are the focus of current work [20].

NGAO R=10 Guide Star	Allocation WFE [nm]	CBE WFE [nm]	CBE Margin [nm]
1. Wavefront Control & Resid. Atm.	**119.6**	**118.0**	19.3
1.1 ASM (fitting, accuracy, latency)	77.7	77.0	10.6
1.3 NGWS (measurement, aliasing, latency)	81.2	79.6	16.2
1.6 OIWFS (measurement, latency)	20.8	20.8	0.0
1.7 OCS (latency, precision)	9.2	9.2	0.0
1.9 Uncorrected Atmospheric Errors	33.7	33.7	0.0
2. Telescope	**63.9**	**54.3**	33.7
2.1 Optical Design	0.3	0.3	0.0
2.2 Telescope Tracking	31.7	17.9	26.1
2.3 M1 figure and alignment	30.7	24.7	18.3
2.4 M2 figure and alignment	40.0	38.5	10.9
2.5 M3 figure and alignment	23.1	23.1	0.0
3. Disturbances	**76.5**	**75.6**	11.7
3.1 Wind Forces	58.0	56.8	11.7
3.2 Mechanical Vibration	31.6	31.6	0.0
3.3 Aero-Thermal	35.6	35.6	0.0
3.4 Gravity and Thermal Flexure	14.9	14.9	0.0
3.5 Atmospheric Refraction	3.0	3.0	0.0
4. Calibration	**46.4**	**46.4**	0.0
4.1 System / ASMS Calibration	22.9	22.9	0.0
4.2 NGWS Calibration	22.4	22.4	0.0
4.4 Instrument Calibration	33.5	33.5	0.0
5. Reserve	**59.5**		
Total WFE	**173.0**	**157.3**	72.0

Wavelength [µm]	1.22	1.65	2.18
Strehl (Allocations)	0.45	0.65	0.78
Strehl (CBE)	0.52	0.70	0.81

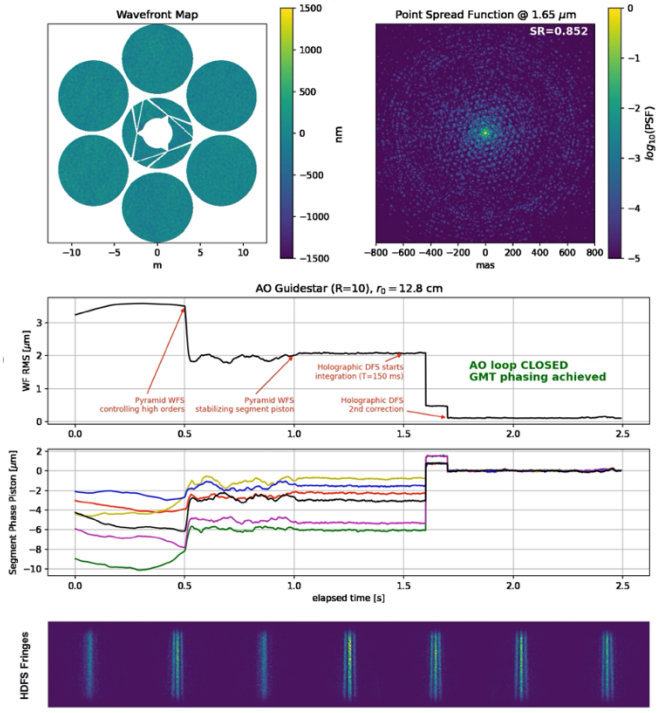

Figure 12: (Left) NGAO wavefront error budget. (Right) Final frame of an NGAO control loop closure simulation.

High-fidelity simulations of NGAO control loop convergence and closed-loop operation with optical and modal gain optimization have recently been performed [21] (Figure 12, right). The sequence includes initially controlling only the continuous modes across each ASM segment to flatten the wavefront in each segment, then closing segment piston using the PWFS, and finally using the HDFS measurements to correct the PWFS phase-wrapping errors. For bright guide stars, this process converges in under 2 s. These same control algorithms are being implemented on the HCAT testbed.

5. LASER TOMOGRAPHY ADAPTIVE OPTICS

5.1 Introduction

The LTAO wavefront control mode uses laser guide stars to enable diffraction-limited observations over a large fraction of the sky. It will be used primarily for high spatial resolution observations of faint extragalactic targets and studies of faint or highly obscured galactic objects such as protostars and substellar objects. The GMT LTAO design uses an asterism of 6 sodium LGS, arranged in a 30″ radius circle surrounding the science target, each sampled by a Shack-Hartmann

wavefront sensor. The measurements of the wavefront sensors are combined tomographically, using prior knowledge of the turbulence strength versus altitude, to estimate the optimal wavefront correction for the cylindrical atmospheric volume towards the science target, which is applied on the ASM.

The LGS cannot be used to measure tip, tilt, and focus aberrations due to the unknown position and range of the illuminated sodium atoms. They also cannot be used to measure segment phase piston error due to the incoherence of the light scattered by those atoms. Finally, changes in the structure and thickness of the sodium layer cause slowly-varying calibration errors (often called LGS aberrations) which must be measured using an NGS. These sensing functions are fulfilled by the On-Instrument Wavefront Sensor (OIWFS) of each diffraction-limited instrument, observing an NGS in the near-infrared. The OIWFS of each instrument differs based on its science case.

The GMTIFS instrument will primarily be used to study faint extragalactic sources, requiring off-axis NGS. It therefore splits the focal plane between a central 20.4×20.4 arcsec square science field and a surrounding 180 arcsec diameter circular OIWFS patrol field. In the absence of any additional wavefront control, the off-axis NGS would suffer from significant anisoplanatism error, reducing the accuracy of the tip-tilt, focus, and segment phase piston measurements. The OIWFS therefore include a 1000-actuator cryogenic deformable mirror that corrects the difference between the estimated on-axis and off-axis wavefronts, both derived from the same LGS measurements.

The GMTNIRS instrument benefits from a simpler OIWFS design. Most GMTNIRS science targets will be point sources sufficiently bright in the near-infrared to use a small fraction (10%) of their light for NGS wavefront sensing. No additional deformable mirror is necessary, as the science target light is corrected by the ASM.

5.2 Laser Guide Star Subsystem

The six LGS required by the LTAO control mode will be generated by the Laser Guide Star Subsystem [22] (LGSS). The LGSS design closely follows that the VLT 4-LGS facility [23], with six independent laser projection units consisting of a 22 W Toptica/MPB SodiumStar laser coupled to a short beam transfer system and refractive launch telescope. The LGS projection units are grouped in pairs at three locations around the perimeter of the M1 mirror (Figure 13, top).

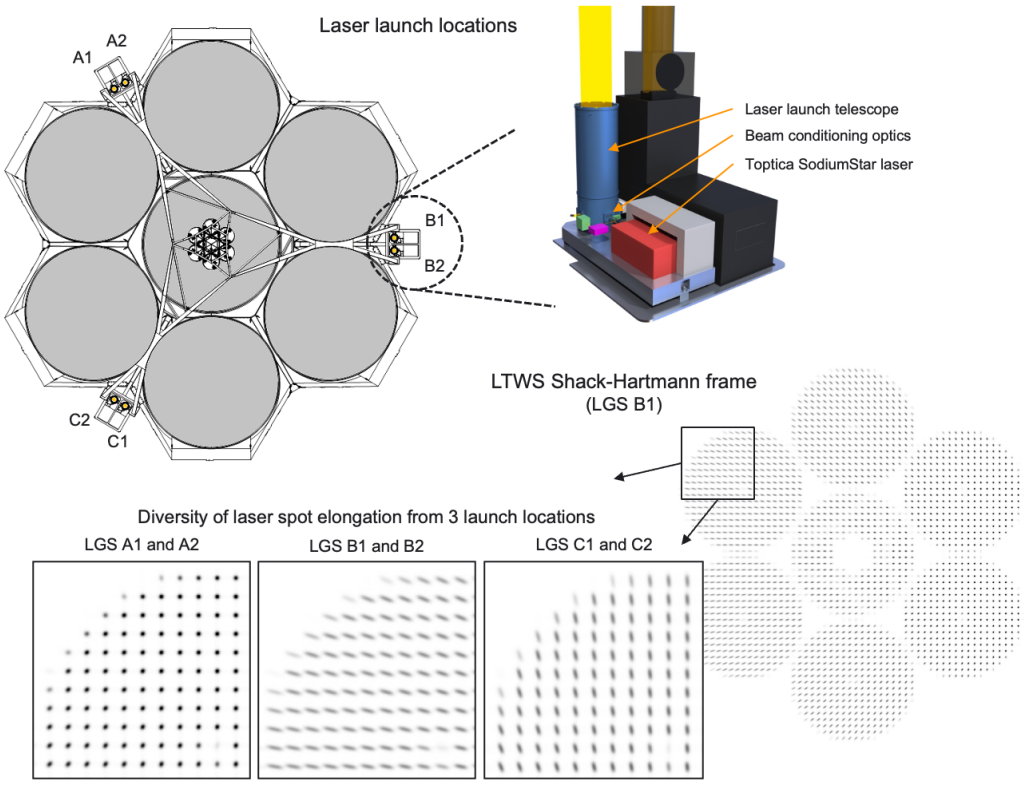

Figure 13: (*Top*) LGSS launch geometry. Lasers are launched in pairs from 3 locations around M1. (*Bottom*) Diversity of LGS spot elongation at every location in the pupil reduces tomography error.

The finite thickness of the mesospheric sodium layer leads to a perspective elongation of the LGS that varies across the pupil as a function of the distance between the wavefront sensor subaperture and the laser launch telescope. Launching the lasers from the perimeter of M1 doubles this perspective elongation compared to launching from behind the secondary mirror. However, this disadvantage is offset by the diversity of the elongation directions that are generated (Figure 13, bottom). Launching from 3 locations around M1 ensures that every location in the pupil is sampled with 3 different elongation directions. Appropriate weighting of the measurements in each axis reduces the tomographic error to a similar level as achieved by launching from the behind the secondary mirror, while enabling a far simpler and lower-risk LGSS design.

5.3 Laser Tomography Wavefront Sensor

The LTWS consists of six 60×60 subaperture Shack-Hartmann wavefront sensors co-mounted in a rotation bearing and on a long-travel focus stage [22] (Figure 14). These stages enable the sensors to track the LGS asterism, which rotates with respect to the sky and instrument, and varies in object range from 83.5 to 190 km. The LTWS preliminary design used the E2V NGSD detector, with 13×13 pixels per subaperture and a field of view of 9.2 arcsec. We now expect to use SONY IMX425 1608×1104 pixel CMOS arrays in FirstLight C-Blue One cameras to provide 14×14 pixels and a field of view of ≥ 9.6 arcsec in each sub-aperture.

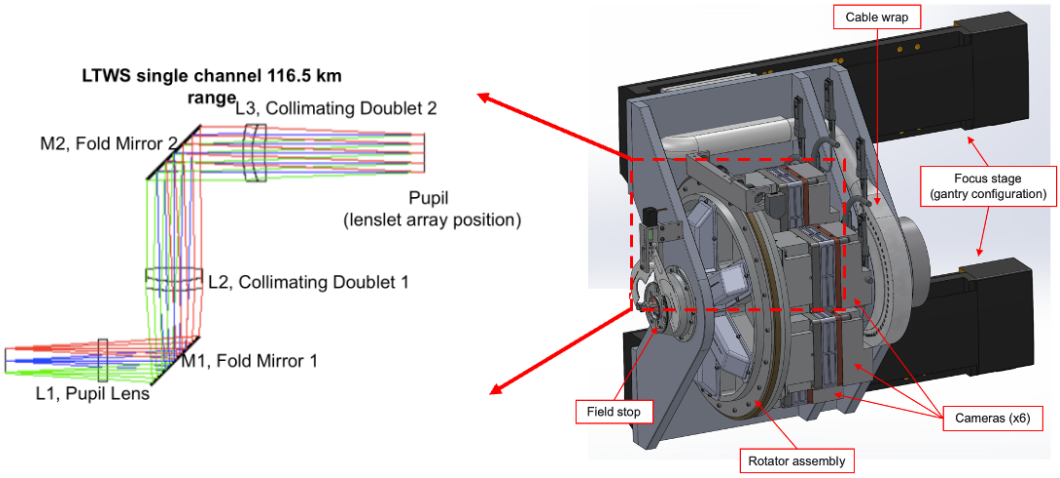

Figure 14: (*Left*) Preliminary optical design of a single channel of the LTWS (*Right*) LTWS preliminary mechanical design.

A delta preliminary design stage for the LGSS and LTWS is expected to begin in late 2023. This will include design updates to conform to telescope interface changes (eg. a change in the facility coolant from ethylene glycol to Novec-7100), and optical design updates to support the higher-performance detectors that are now available.

5.4 On-Instrument Wavefront Sensor

The LTWS Shack-Hartmann wavefront sensors measure local wavefront slope and are blind to phase differences across pupil discontinuities. They are also unable to measure global tip-tilt and focus due to the variable position and range of the LGS, and prone to slowly-varying calibration errors due to sodium layer profile changes and spot truncation. The OIWFS must therefore measure global tip/tilt and segment phase piston error at 50-500 Hz, focus error at 10 Hz, and ~100 higher-order modes at 0.1 Hz.

Both the GMTNIRS and GMTIFS OIWFS use sequential phase retrieval to measure segment piston errors from Nyquist-sampled K band images of the guide star [24]. This real-time phase retrieval approach is enabled by low-noise, high-frame rate eAPD detector arrays and the high-order AO correction provided by the high-bandwidth LTAO control loops. Our baseline approach is to use the Gerchberg-Saxton algorithm [25] to iteratively solve for the wavefront error that generated the observed images, sampled at 500 Hz. The phase reconstruction is done on a 30×30 grid of points in the pupil, which are then projected onto tip, tilt, focus, and segment phase piston modes. While this method meets our requirements, other phase retrieval algorithms such as Fast and Furious [26] are also being investigated to evaluate whether they might provide similar accuracy with lower computational demands.

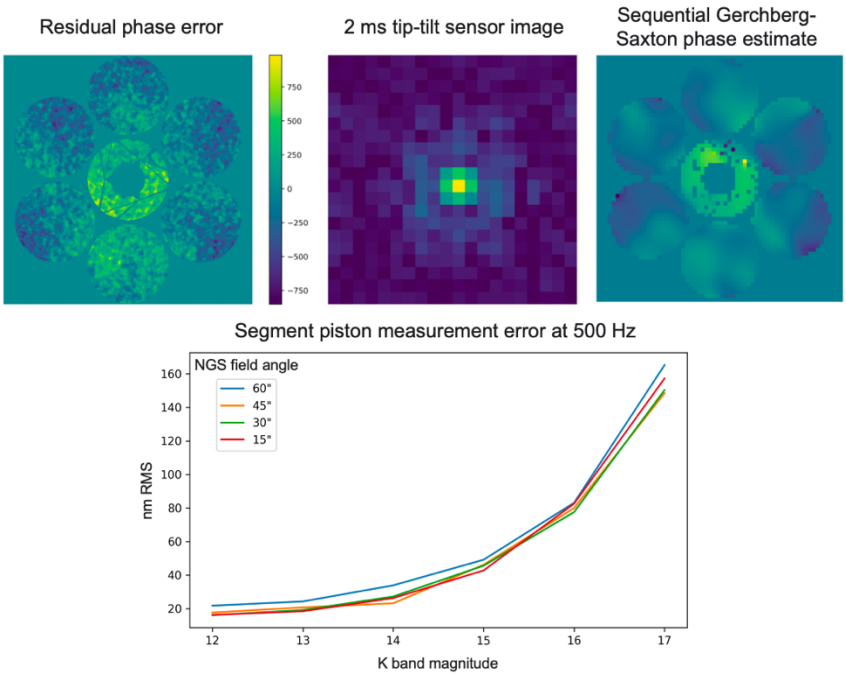

Figure 15: (*Top*) Phase retrieval using a simulated 2 ms tip-tilt sensor integration of a K=14 guide star. (*Bottom*) Expected segment piston measurement error as a function of OIWFS guide star magnitude and field angle.

Focus and slowly-varying higher-order calibration errors will be sensed using Shack-Hartmann sensors in each OIWFS. GMTNIRS will use an H band 20×20 Shack-Hartmann sensor to measure higher-order errors, while GMTIFS will have an H band 2×2 focus sensor and a J band 24×24 dynamic calibration sensor. The measured focus error is applied via an integrator to the LTWS focus stage, while the residual low-order aberrations are applied as updates to the centroid reference vector of the LTWS. The on-axis tomography control loop responds to these changes and applies the corrections to the ASM at ≥ 500 Hz.

5.5 LTAO Expected Performance

As for NGAO, an analytic wavefront error budgets are used to flow down performance requirements to subsystems and compute the CBE performance in the LTAO control mode. Each term represents the median image quality degradation due to that source of error over the likely observing conditions (the GMT Standard Year [27]). Two budgets are maintained, representing the key performance requirements for the GMTNIRS and GMTIFS instruments. The budget corresponding to GMTIFS image quality at 80% sky coverage is illustrated in Figure 16, left. CBEs highlighted in green are based on simulations or analyses that represent the current design or as-built components, with statistical analyses over likely environmental conditions using the Standard Year framework where appropriate. CBEs highlighted in yellow are equal to the allocations and have not yet been confirmed. The estimates derived from the current designs and as-built components comprise 90% of the total variance.

The dominant error term at high sky coverage is OIWFS measurement error. This was estimated as follows:

- LTAO simulations including all major error sources (median atmospheric fitting, LTWS measurement, tomography, median wind disturbance, NGS wavefront sensing, latency) were run for a grid of NGS magnitudes ($10 < K < 20$) and off-axis distances ($0'' < r < 90''$), deriving the total residual wavefront error.
- 1000 science target coordinates were selected at random from the Standard Year database, and all stars with $K < 20$ within 90″ of the science target extracted from the GAIA catalogue.
- The WFE versus magnitude and off-axis distance grid was bi-linearly interpolated for each potential guide star, and the best guide star selected.
- The 1000 science targets were sorted by the WFE expected when using the best guide star, to compute the expected wavefront error versus percentile sky coverage.

LTAO 80% Sky Coverage	Allocation	CBE	
	WFE [nm]	WFE [nm]	Margin [nm]
1. Wavefront Control & Resid. Atm.	**295.6**	**279.2**	97.0
1.1 ASMS (fitting, accuracy, latency)	95.1	95.8	-11.8
1.2 AGWS (low-bandwidth phasing)	0.0	0.0	0.0
1.4 LTWS (fitting, meas., latency)	116.6	116.3	8.6
1.5 TMS (high-bandwidth phasing)	63.2	49.7	39.1
1.6 OIWFS (tip-tilt, focus, phasing)	199.8	181.2	84.1
1.7 OCS (latency, precision)	9.2	9.2	0.0
1.8 Tomography Error	140.0	135.0	37.1
1.9 Uncorrected Atmospheric Errors	33.7	40.5	-22.5
2. Telescope	**60.7**	**53.5**	28.6
2.1 Optical Design	0.3	0.3	0.0
2.2 Telescope Tracking	31.7	21.3	23.5
2.3 M1 figure and alignment	30.7	26.7	15.1
2.4 M2 figure and alignment	34.6	34.1	6.0
2.5 M3 figure and alignment	23.1	23.1	0.0
3. Disturbances	**119.4**	**104.1**	58.6
3.1 Wind Forces	90.4	67.6	60.1
3.2 Mechanical Vibration	31.6	31.6	0.0
3.3 Aero-Thermal	69.7	69.7	0.0
3.4 Gravity and Thermal Flexure	14.9	14.9	0.0
3.5 Atmospheric Refraction	3.0	13.8	-13.5
4. Calibration	**46.4**	**46.4**	0.0
4.1 System / ASMS Calibration	22.9	22.9	0.0
4.3 LTWS Calibration	22.4	22.4	0.0
4.4 Instrument Calibration	33.5	33.5	0.0
5. Reserve	**90.3**		
Total WFE	**340.0**	**306.3**	147.6

Wavelength [µm]	1.22	1.65	2.18
Strehl (Allocations)	0.17	0.30	0.43
Strehl (CBE)	0.21	0.35	0.48

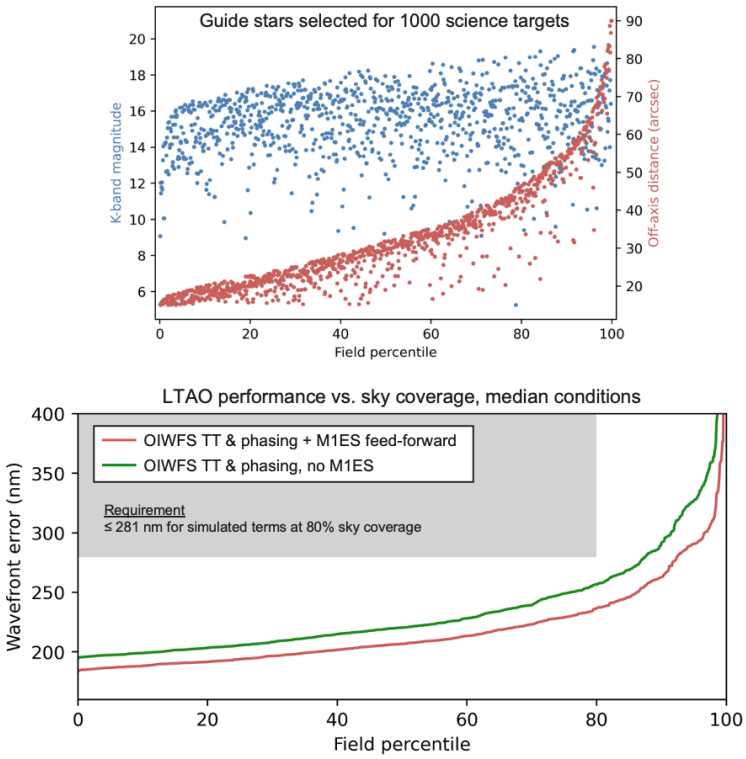

Figure 16: (*Left*) LTAO 80% sky coverage wavefront error budget. (*Top right*) OIWFS guide star K magnitude and off-axis distance as a function of sky coverage. (*Bottom right*) Wavefront error as a function of sky coverage derived from simulation of major error terms.

The wavefront error versus sky coverage for the simulated error terms, for two potential control architectures, is illustrated in Figure 16, bottom right. The green light represents the total WFE if controlling segment piston error only based on OIWFS feedback, while the red line adds feed-forward control from the M1 Edge Sensors, part of the TMS. Both designs meet requirements (< 281 nm RMS at 80% sky coverage for the error terms simulated), but the edge sensor feed-forward loop provides a clear benefit in all cases. Adding all other error terms, we predict Strehl(1.65 µm) = 0.35 at 80% sky coverage in median conditions, compared to a requirement of ≥ 0.30.

6. CALIBRATION, INTEGRATION, AND TESTING

6.1 Wavefront Control Calibration Subsystem

The Wavefront Control Calibration Subsystem (WCCS) consists optical calibration sources that can be inserted at the telescope prime focus, and a metrology interferometer located at the folded Gregorian focus. These components will be used during telescope commissioning and in daytime during regular operations to calibrate the ASM and AO wavefront sensors. The prime focus optical modules consist of an NGS module replicating the light of an on-axis NGS, an LTAO module replicating the light of the 6 laser guide star asterism and an on-axis NGS, and a retro-reflector module used with the M2 Interferometer. Each can be deployed to the prime focus of the telescope on an actuated arm (Figure 17, top).

6.2 AO Integration Facility

The adaptive optics subsystems of the GMT will first be integrated and tested on the Adaptive Optics Integration Facility (OAIF, Figure 17, bottom). The AOIF consists of the ASM on a test stand, the AO Test Camera (a Nyquist-sampled infrared camera with a prototype On-Instrument Wavefront Sensor), the NGWS and LTWS wavefront sensors, and the WCCS optical modules. This facility will initially be deployed at ADS International in Lecco, Italy for integrated AO testing as ASM segments are completed, then moved to the observatory for final acceptance testing of all subsystems and system-level performance verification.

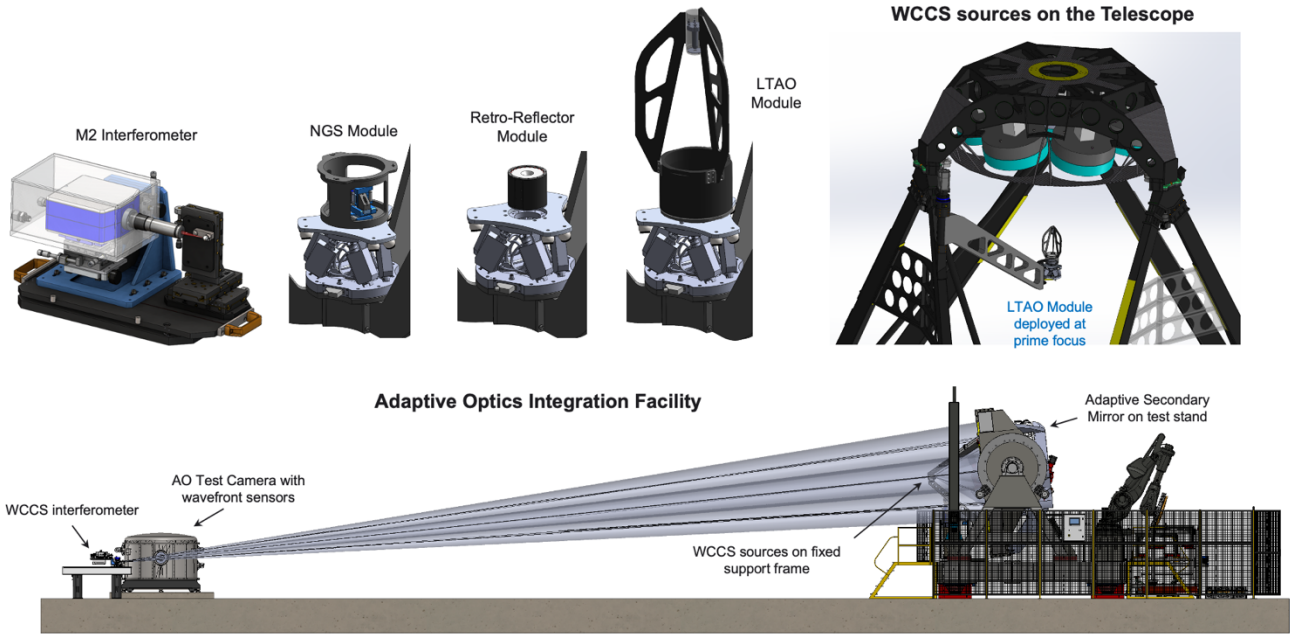

Figure 17: (*Top left*) Wavefront Control Calibration Subsystem component. These can be mounted on the telescope (*top right*) or used in the Adaptive Optics Integration Facility (*bottom*).

7. SUMMARY

We have provided a comprehensive update on the status of the GMT adaptive optics system. Most AO subsystems are in the final design and/or prototyping phases. The adaptive secondary mirror is in fabrication, with the main components of the first off-axis segment completed. The approach for initially aligning and maintaining the GMT segments phased has matured, with updates to several wavefront sensors. The NGAO pyramid wavefront sensor now includes an HDFS second channel to unambiguously correct phase wrapping errors of the pyramid wavefront sensor. We have also adopted a new design for actively maintaining segment phasing in the LTAO mode. Segment piston will be measured using sequential phase retrieval in the OIWFS tip-tilt sensor, enabling high-bandwidth closed-loop segment phasing, even when using faint NGS at high sky coverage.

These design updates have been supported by a significantly increased fidelity in system-level wavefront control simulations. This includes simulating the acquisition and control loop convergence processes, the dynamic interaction between control loops and telescope structures, and soft real-time processes such as control loop optimization. They are also supported by two new system-level optical testbeds that are being used to evaluated prototype wavefront sensor performance and test control algorithms. The Wide Field Phasing Testbed is focused on active optics and initial alignment and phasing of the GMT, while the High Contrast AO Testbed is verifying wavefront control and fine phasing in the NGAO mode.

REFERENCES

[1] J. Fanson et al., "Overview and status of the Giant Magellan Telescope project," Proc. SPIE 12182, 121821C (2022).

[2] W. Burgett et al., "The Giant Magellan Telescope mount: the core of a next generation 25.4-m aperture ELT," Proc. SPIE 12182, 121821G (2022).

[3] A. Szentgyorgyi et al., "The GMT-consortium large earth finder (G-CLEF): an optical echelle spectrograph for the Giant Magellan Telescope (GMT)," Proc. SPIE 10702, 107021R (2018).

[4] D. L. DePoy et al., "GMACS: a wide-field, moderate-resolution spectrograph for the Giant Magellan Telescope," Proc. SPIE 10702, 107021X (2018).

[5] J. Lawrence et al., “The MANIFEST pre-concept design,” Proc. SPIE 11447, 1144728 (2020).

[6] R. Sharp et al., “Design evolution of the Giant Magellan Telescope Integral Field Spectrograph, GMTIFS,” Proc. SPIE 10702, 107021V (2018).

[7] D. T. Jaffe et al., “GMTNIRS: progress toward the Giant Magellan Telescope near-infrared spectrograph,” Proc. SPIE 9908, 990821 (2016).

[8] M. Kautz et al., “GMagAO-X: A First Light Coronagraphic Adaptive Optics System for the GMT,” AO4ELT7 proceedings (2023).

[9] J. D. Crane et al., “Conceptual design of the Giant Magellan Telescope commissioning camera,” Proc. SPIE 11447, 114472J (2020).

[10] B. N. Sitarski et al., “The GMT telescope metrology system design,” Proc. SPIE 12182, 1218207 (2022).

[11] B. McLeod et al., “The acquisition, guiding, and wavefront sensing system for the Giant Magellan Telescope,” Proc. SPIE 10700, 107001T (2018).

[12] B. McLeod et al., “The wide field phasing testbed for the Giant Magellan Telescope,” Proc. SPIE 12182, 1218208 (2022).

[13] D. Gallieni et al., “GMT adaptive secondary mirrors subsystem final design,”, Proc. SPIE 11448, 114485K (2020).

[14] C. Plantet et al., “NGWS-P: the natural guide star wavefront sensor prototype of GMT single conjugate AO system NGAO,” Proc. SPIE 12185, 121854H (2022).

[15] A.-L. Cheffot et al., “Differential piston sensing with LIFT: application to the GMT,” Proc. SPIE 12185, 1218557 (2022).

[16] S. Y. Haffert et al., “The Holographic Dispersed Fringe Sensors (HDFS): phasing the Giant Magellan Telescope,” JATIS 8, 021513 (2022).

[17] A. D. Hedglen at al., “Lab tests of segment/petal phasing with a pyramid wavefront sensor and a holographic dispersed fringe sensor in turbulence with the Giant Magellan Telescope high contrast adaptive optics phasing testbed,” JATIS 8, 021515 (2022).

[18] L. Close et al., “The 21,000 Actuator GMagAO-X Parallel DM for the Giant Magellan Telescope: First HCAT Testbed Results with Segment/Petal phasing/AO control of Seven GMT Segments,” AO4ELT7 Proceedings (2023).

[19] C. Plantet et al., “Integration and first tests of the Natural Guide Star Wavefront Sensor Prototype for GMT,” AO4ELT7 Proceedings (2023).

[20] R. Conan et al., “GMT NGAO Integrated Modeling,” AO4ELT7 Proceedings (2023).

[21] F. Quirós-Pacheco et al., “Phasing the GMT in the Natural Guide star Adaptive Optics mode: from simulations to testbeds,” AO4ELT7 Proceedings (2023).

[22] R. Conan et al., “The Giant Magellan Telescope laser tomography adaptive optics system,” Proc. SPIE 9447, 84473P (2012).

[23] W. Hackenberg et al., “Assembly and test results of the AOF laser guide star units at ESO,” Proc. SPIE 9148, 91483O (2014).

[24] M. van Dam at all., “Segment piston estimation using sequential phase retrieval,” AO4ELT7 Proceedings (2023).

[25] R.W. Gerchberg and W.O. Saxton, “A practical algorithm for the determination of the phase from image and diffraction plane pictures,” *Optik*. 35: 237–246 (1972)

[26] V. Korkiakoski et al., “Fast & Furious focal-plane wavefront sensing,” *Applied Optics* 53.20, 4565-4579 (2014).

[27] B. Sitarski et al., “Performance Estimates for the Giant Magellan Telescope via Statistical Analysis,” AO4ELT6 Proceedings (2019).